Forest Ecology and Management 310 (2013) 968–982

Contents lists available at ScienceDirect

Forest Ecology and Management

journal homepage: www.elsevier.com/locate/foreco

Propagating uncertainty to estimates of above-ground biomass for Kenyan mangroves: A scaling procedure from tree to landscape level

R. Cohen [a,*], J. Kaino [b], J.A. Okello [b,c], J.O. Bosire [b], J.G. Kairo [b], M. Huxham [d], M. Mencuccini [a]

[a] School of Geosciences, University of Edinburgh, Crew Building, West Mains Road, Edinburgh EH9 3JN, United Kingdom
[b] Kenya Marine and Fisheries Research Institute, P.O. Box 81651, Mombasa, Kenya
[c] Department of Plant Biology and Nature Management (APNA), Vrije Universiteit Brussels, Pleinlaan 2, 1050 Brussels, Belgium
[d] School of Life, Sport and Social Sciences, Edinburgh Napier University, Edinburgh, United Kingdom

ARTICLE INFO

Article history:
Received 17 June 2013
Received in revised form 20 September 2013
Accepted 22 September 2013
Available online 20 October 2013

Keywords:
Above-ground biomass
Mangrove
Allometric equations
Uncertainty propagation
Mixed-effects models
Kenya

ABSTRACT

Mangroves are globally important carbon stores and as such have potential for inclusion in future forest-based climate change mitigation strategies such as Reduced Emissions from Deforestation and Degradation (REDD+). Participation in REDD+ will require developing countries to produce robust estimates of forest above-ground biomass (AGB) accompanied by an appropriate measure of uncertainty. Final estimates of AGB should account for known sources of uncertainty (measurement and predictive) particularly when estimating AGB at large spatial scales. In this study, mixed-effects models were used to account for variability in the allometric relationship of Kenyan mangroves due to species and site effects. A generic biomass equation for Kenyan mangroves was produced in addition to a set of species-site specific equations. The generic equation has potential for broad application as it can be used to predict the AGB of new trees where there is no pre-existing knowledge of the specific species-site allometric relationship: the most commonly encountered scenario in practical biomass studies. Predictions of AGB using the mixed-effects model showed good correspondence with the original observed values of AGB although displayed a poorer fit at higher AGB values, suggesting caution in extrapolation. A strong relationship was found between the observed and predicted values of AGB using an independent validation dataset from the Zambezi Delta, Mozambique ($R^2 = 0.96$, $p = < 0.001$). The simulation based approach to uncertainty propagation employed in the current study produced estimates of AGB at different spatial scales (tree – landscape level) accompanied by a realistic measure of the total uncertainty. Estimates of mangrove AGB in Kenya are presented at the plot, regional and landscape level accompanied by 95% prediction intervals. The 95% prediction intervals for landscape level estimates of total AGB stocks suggest that between 5.4 and 7.2 megatonnes of AGB is currently held in Kenyan mangrove forests.

1. Introduction

Mangrove forests are now widely recognised as globally important carbon (C) stores (Bouillon et al., 2008; Chmura et al., 2003; Donato et al., 2011; McKee et al., 2007). Despite accounting for just 0.7% of the world's tropical forest cover (Giri et al., 2011) mangroves play a disproportionately important role in the global C cycle. Recent estimates suggest that as much as 20Pg of C is currently being stored in mangrove biomass, sediments and peat world-wide (Donato et al., 2011). Mangroves do not merely sequester and store C they also provide a number of other key ecosystem services which are ecologically and economically important at local, regional and global scales. Such services include but are not limited to; coastal defence (Zhang et al., 2012), fisheries production (Aburto-Oropeza et al., 2008), habitat provision for terrestrial and aquatic fauna (Kathiresan and Bingham, 2001), timber and fuelwood production (Dahdouh-Guebas et al., 2000), pollution abatement (Wickramasinghe et al., 2009) and regulation of sediment exchange between land and sea (Duarte et al., 2005).

The continued degradation and destruction of mangroves world-wide has been highlighted in recent years (Alongi, 2002; Giri et al., 2011). Mangroves are considered to be one of the most threatened ecosystems on the planet with an estimated decline in global cover of ~35% during the period 1980–2000 (Valiela et al., 2001). This decline is largely due to over-exploitation of wood products, conversion to aquaculture, coastal development and human settlement (Primavera, 2005). Although rates of destruction may be slowing in some countries they generally remain high; for example Kenya experienced an estimated mean loss of mangrove cover of ~0.7% yr^{-1} during the period 1985–2010

* Corresponding author. Tel.: +44 (0) 131 650 5103.
E-mail address: Rachel.Cohen@ed.ac.uk (R. Cohen).

0378-1127
http://dx.doi.org/10.1016/j.foreco.2013.09.047

(Kirui et al., 2012). Continued degradation and loss of mangrove cover not only represents a loss of future C sequestration potential but could result in significant release into the atmosphere of C currently being stored by mangroves (Pendleton et al., 2012).

An estimated 8–20% of annual global anthropogenic CO_2 emissions result from land-use changes occurring primarily in the tropics (van der Werf et al., 2009). This realisation has led to proposals for forest-based climate change mitigation strategies such as Reduced Emissions from Deforestation and Degradation (REDD+). In essence REDD+ envisages achieving CO_2 emissions reductions, forest conservation and sustainable development by placing an economic value on forest carbon storage and facilitating the transfer of funds from developed to developing nations through international trade in carbon credits. Details of how REDD+ will operate at the national and international level under the United Nations Framework Convention for Climate Change (UNFCCC) are still under debate. However many developing nations (including Kenya) are already in the process of formulating national REDD+ readiness strategies in partnership with the World Bank's Forest Carbon Partnership Facility (FCPF). There is definite scope for mangroves to be included in national and/or local scale forest carbon projects operating either under existing voluntary or future compliance carbon markets. Indeed, a recent study by Siikamaki et al. (2012) suggested that at the global scale reducing CO_2 emissions by avoiding further loss of mangroves could prove to be an economically viable option in comparison with the cost of reducing emissions from other sources (e.g. industry) even under scenarios of low mangrove carbon offset supply.

Participation in REDD+ (under the UNFCCC) will require countries to produce accurate estimates of their forest carbon stocks and stock changes through robust Measurement, Reporting and Verification (MRV) programs. The most recent Intergovernmental Panel on Climate Change (IPCC) Guidelines for National Greenhouse Gas Inventories (IPCC, 2006) provide the current methodological framework for REDD+ MRV requirements (Maniatis and Mollicone, 2010). In accordance with these guidelines all estimates should be accompanied by an appropriate measure of uncertainty (95% confidence interval) and should account for and reduce all known sources of uncertainty as far as is possible (IPCC, 2006). Above-ground biomass (AGB) is one of five forest carbon pools (identified by the IPCC) which will be estimable and reportable for REDD+. Providing robust estimates of AGB is important both in terms of future REDD+ reporting but also in providing the link between ground and remote sensing efforts to monitor changes in forest biomass and land cover at local, regional and global scales.

The above-ground biomass of trees is commonly estimated by the use of allometric equations (derived using regression analysis) which relate one or more easily measurable tree variables (e.g., stem diameter at breast height (DBH)) to total above-ground biomass. These equations are then applied to forest inventory data in order to estimate biomass at larger spatial scales. Allometric equations have been developed for a variety of mangrove species occurring across a broad geographical range (Clough and Scott, 1989; Kairo et al., 2009; Komiyama et al., 2005; Poungparn et al., 2002; Soares and Schaeffer-Novelli, 2005). However, African mangroves are under-represented in the current literature with published equations existing for Kenya (Kairo et al., 2009; Kairo et al., 2008; Kirui et al., 2006; Slim et al., 1996; Tamooh et al., 2009) and South Africa (Steinke et al., 1995) only.

Allometric relationships in trees are generally considered to be both species and site-specific. However, the infeasibility of constructing a new allometric equation for every species encountered at every new site has led to increasing interest in the development of generic equations for biomass estimation (Brown et al., 1989; Chave et al., 2005; Zianis and Mencuccini, 2004). Existing generic equations for mangroves have used wood density as the species-specific component of the relationship (Chave et al., 2005; Komiyama et al., 2005). The generic equation developed by Komiyama et al. (2005) was deemed to perform within acceptable levels of precision (as measured by the relative error) in comparison with site-specific equations for selected species (Komiyama et al., 2008).

Uncertainties are introduced at all stages of the biomass estimation process (from single tree to landscape level). Total uncertainty at the single tree level is comprised of uncertainty in the measurement of tree variables (measurement uncertainty) and uncertainty due to the use of the allometric model for predicting the biomass of a new individual (predictive uncertainty) (Chave et al., 2004; Zianis, 2008). These uncertainties are, in turn, propagated to plot and landscape level biomass estimates. Failing to account for uncertainty during the biomass estimation process ultimately leads to an underestimation of the uncertainty on final predictions (Dietze et al., 2008).

Accounting for predictive uncertainty is particularly important in biomass estimation as allometric equations are often applied outwith the data range for which they were originally intended (Chave et al., 2005) and are always applied outside the particular trees (and often sites) from which they were developed. Uncertainty in the parameters of a regression model is often represented by simply quoting the standard error of the allometric constants whilst the coefficient of determination (R^2) is the usual means by which to evaluate both the 'fit' of the model and its predictive power (e.g. Komiyama et al., 2005; Soares and Schaeffer-Novelli, 2005). However, over reliance on the use of R^2 in regression analysis as a measure of model predictive accuracy and for model comparison (between datasets) has been criticised in recent years (Gelman and Pardoe, 2006; Johnson and Omland, 2004). In contrast to model selection criteria such as the Akaike Information Criteria (AIC) (Akaike, 1987) the R^2 statistic is not a direct measure of model predictive accuracy and model selection made solely on the basis of maximising the R^2 statistic can lead to imprecise predictions as no account is taken of model complexity (Johnson and Omland, 2004).

The issue of uncertainty in biomass estimation has been addressed in the literature for forests in general (Brown, 2002; Chave et al., 2004; Ketterings et al., 2001; Parresol, 1999; Phillips et al., 2000; Zianis, 2008). Methodologies for propagating uncertainty have been presented based on summing the variances of component sources of uncertainty (see Chave et al., 2004; Ketterings et al., 2001; Phillips et al., 2000) and simulation techniques such as Monte Carlo (Heath and Smith, 2000; Ryan, 2009). To the best of our knowledge such methodologies have never been applied for the purpose of propagating uncertainty to biomass estimates in mangroves. With this in mind and in the context of future REDD+ requirements for biomass/carbon accounting this study focused on: (1) the development of new allometric equations to estimate the above-ground biomass of Kenyan mangroves using linear mixed-effects models and based on a meta-analysis of all the available harvest data for Kenyan mangrove species (2) demonstrating a simulation based methodology for propagating uncertainty during the biomass estimation process and (3) demonstrating the practical application of said equations and simulations to a large forest inventory dataset spanning the entire Kenyan coastline for the purpose of producing estimates of above-ground biomass at different spatial scales (tree, plot, region and landscape) with an appropriate measure of uncertainty.

2. Methods

2.1. Harvest dataset – model development and validation

The harvest data used in this study is detailed in Table 1 and represents the largest dataset compiled to date for African

mangroves. The bulk of the harvest data originates from the Gazi Bay area (4°25′S, 39°30′E) located ~55 km south of the city of Mombasa in Kenya (Fig. 1) and was made available through collaboration with Kenya Marine and Fisheries Research Institute (KMFRI). The Gazi Bay data has been divided into two sub-sites; Gazi (the area next to Gazi village) and Kinondo (the area next to Kinondo village). An additional study within the Gazi Bay area by Slim et al. (1996) was considered for inclusion but discounted as it was not possible to obtain the raw data. Attempts were made to source additional datasets from outwith Africa in order to expand the range of stem diameter and height data available for each species and also to provide some data for species (e.g. *Xylocarpus* sp.) not included in any of the African studies. An extensive literature search was carried out to look for raw harvest data which were (1) from the same species that occur in Kenya and (2) freely available in the publication. It was only possible to find one study which met both these criteria; that of Poungparn et al. (2002) from South-East Asia.

The harvest dataset used in this study to develop regression models comprises the raw data from 337 individually harvested trees (see Section 2.1.1 for harvest methodology) and includes data for seven of the nine mangrove species known to occur in Kenya. The harvest dataset is unbalanced with very few data points for some species (Table 1). However, *Rhizophora mucronata* and *Avicennia marina* are well represented in the dataset in terms of sample size and these are two of the most dominant and widely distributed mangrove species in Kenya. In common with most allometric studies, there is a paucity of data from large diameter size classes with 97% of the harvested trees in the current dataset <20 cm in diameter. This means that the data range in the harvest dataset does not fully encompass the upper values of diameter and height recorded in the existing forest inventories.

Harvest data from a recent study conducted by WWF, Mozambique and KMFRI in 2011 in the Zambezi Delta, Mozambique (Bosire et al., unpublished results) were used in this study for validation purposes only and were not used to develop regression models (data summarised in Table 1). The Zambezi validation dataset comprises harvest data from 23 trees from six mangrove species occurring in both Mozambique and Kenya.

2.1.1. Summary of harvest methodology

All of the studies listed in Table 1 employed similar methodologies for tree harvesting and determination of total live above-ground biomass (but see individual papers for details). Harvested trees were selected randomly and prior to harvest, the stem diameter (cm) and total height (m) of each tree was recorded. Stem diameter was measured at 1.3 m above-ground (DBH) except in the case of *Rhizophora* trees where the highest prop root occurred >1.3 m above-ground in which case diameter was measured at ~30 cm above the highest prop root. Trees were then harvested at ground level and the fresh weight of component parts (stem, branches, leaves and prop roots in the case of *Rhizophora* sp.) was measured in the field. Sub-samples of component parts were then oven dried to constant weight (80–85 °C in the case of all studies apart from Poungparn et al. (2002) where fresh material was dried at 110 °C) in order to calculate wet-dry weight ratios (conversion factors). Conversion factors were then applied to convert the fresh weight of each tree component to dry weight in kilograms (kg DW) and summed giving total above-ground biomass in kg DW. The study by Kirui (2006) employed a slightly different methodology for determining the total above-ground biomass of multi-stemmed *Avicennia* trees. Each stem arising from a common butt was treated as an individual tree and the biomass of each stem was calculated separately following a procedure outlined in Clough et al. (1997) involving apportionment of the common butt.

2.2. Statistical analyses

2.2.1. Rationale for using mixed-effects models

Ecological datasets often display a complex structure where data from individuals within populations are nested or grouped by one or more factors. Such grouping factors could include for example; the species and/or site which the individual belongs to, an experimental treatment applied to a subset of individuals and time series data. If such correlations or group effects are not accounted for during analysis the standard errors of the regression coefficients will tend to be underestimated due to inflation of the effective sample size (Steele, 2008). Mixed-effects models not only account for but explicitly model the variance due to group effects.

In mixed-effects models the intercept and regression coefficients can be assigned their own probability models and allowed to vary by group (as random effects) around the overall population mean (the fixed effects). This is particularly useful in studies where the main target of inference is the wider population and predictions are sought for new individuals within new groups, with an appropriate measure of predictive uncertainty (Gelman and Hill, 2007). In addition, mixed-effects models deal well with unbalanced datasets (especially common in meta-analysis studies) and provide a more robust estimation of regression coefficients for groups where there is little information (i.e. a small sample size) as additional information on the probability distribution of coefficients can be gained from the dataset as a whole (Dietze et al., 2008).

2.2.2. Model specification and selection process

The power function equation (Eq. (1)) or its linearized form (Eq. (2)) is commonly used as the underlying allometric scaling relationship for biomass regression models (e.g. Brown et al., 1989; Chave et al., 2005; Komiyama et al., 2008; Parresol, 1999).

$$y = ax^b \tag{1}$$

$$\ln(y) = \ln(a) + b\ln(x) + e_i \tag{2}$$

where y is the response variable, x is the predictive variable and a and b are the allometric constants. Specifically, a is the scaling coefficient (or intercept), b is the scaling exponent (or slope) and e_i is the error term which is assumed to be normally distributed $e^i \sim N(0, \sigma^2)$. For mangroves, biomass regression models have been developed using stem diameter (D) as the sole predictive variable (Clough and Scott, 1989; Steinke et al., 1995). However, many studies have found that the inclusion of additional biometric variables (e.g. tree height (H)) either fitted independently or as a combined variable such as $x = D * H$ or $x = D^2 * H$ have improved model fit (Chave et al., 2005; Komiyama et al., 2002; Soares and Schaeffer-Novelli, 2005). The inclusion of wood density as a predictive variable in models has also been recommended (Chave et al., 2005; Komiyama et al., 2005).

In the current study, a linear relationship was obtained between predictive variables (diameter and height) and the response variable (total above-ground biomass (AGB)) after transforming all variables by natural log (Fig. 2) allowing for the use of regression models of the form shown in Eq. (2). Wood density was not included as a potential predictive variable as tree level wood density data were not available in the harvest dataset used for model development. The individual level grouping factor used in the current study was a combined species_site indicator which grouped the harvest data from individuals within each species at each site in the dataset. For example data from *Rhizophora* trees at Kinondo (Table 1) formed the group Rhiz_Kin and so on. In total there were eighteen species_site groupings present within the harvest dataset. It was necessary to combine species and site into one grouping

Table 1
Provenance and summary of the tree harvest dataset used in this study to develop and validate biomass equations for Kenyan mangroves.[a]

Study	Location	Forest type	Species	Stem diameter range (cm)	Height range (m)	Above-ground biomass (kg DW)	Sample size
Lang'at (2008)	Ramisi, Kenya	Plantation (12 yrs old)	*Bruguiera gymnorrhiza*	1.1–4.8	2.7–6.6	0.5–7.3	15
Kairo et al. (2008)	Kinondo (Gazi Bay), Kenya	Plantation (12 yrs old)	*Rhizophora mucronata*	2.4–11.5	3.5–8.9	0.6–68.9	50
Kirui et al. (2006)	Gazi (Gazi Bay), Kenya	Natural	*Rhizophora mucronata*	5.7–21.4	4.3–11.3	13.4–269.5	15
Kirui (2006)	Kipini, Kenya	Natural	*Rhizophora mucronata*	2.3–23.6	2.8–16.1	0.6–383.7	15
			Avicennia marina	2.5–15.8	3.9–11.7	4.6–71.4	28 (19)
	Gazi (Gazi Bay), Kenya	Natural	*Avicennia marina*	3.7–21.8	2.1–11.3	7.2–127.3	51 (15)
Tamooh et al. (2009)	Gazi (Gazi Bay), Kenya	Plantation (6yrs old)	*Rhizophora mucronata*	0.9–6.4	0.8–3.9	0.08–16.2	12
Kairo et al. (2009)	Gazi (Gazi Bay), Kenya	Plantation[b]	*Avicennia marina*	5.2–10.2	4–5.8	6.8–22.5	10
			Sonneratia alba	5.3–11.3	4–5	3.8–9.4	10
			Ceriops tagal	5–5.5	1.8–2.6	1.5–6.1	10
			Rhizophora mucronata	3–8	2.8–5	3–25.8	58
Steinke et al. (1995)	Mgeni estuary, South Africa	Natural	*Bruguiera gymnorrhiza*	3.4–11.5	4.6–13.5	3.2–107.2	12
			Avicennia marina	5.4–9.9	4.9–7.7	5.3–31.9	4
Poungparn et al. (2002)	Thailand	Natural	*Sonneratia alba*	4.2–12.7	3.4–13.4	3.1–79.3	10
			Bruguiera gymnorrhiza	4.8–33.4	9.2–24.9	8.3–943.5	10
			Rhizophora mucronata	4.7–11.2	6.9–16	7.7–73.7	11
			Xylocarpus granatum	3.7–12.7	4.1–8	3.2–66.8	8
	Indonesia	Natural	*Sonneratia alba*	6.7–21.7	7.3–22.6	13.1–256	2
			Bruguiera gymnorrhiza	9.7–48.9	11.1–30.6	54.7–1411.1	4
			Xylocarpus granatum	18.6	13.4	162.2	1
			Xylocarpus moluccensis	11.8	13.5	47.4	1
WWF/KMFRI (Validation Dataset)	Zambezi Delta, Mozambique	Natural	*Ceriops tagal*	5.3–15.4	3.6–6.5	6.55–68.2	3
			Bruguiera gymnorrhiza	5.6–24.6	5.5–8.1	11.7–161.8	4
			Xylocarpus granatum	5.2–14.9	4–7.8	6.7–49	3
			Sonneratia alba	5.9–35	5.9–13.5	8.8–453.4	6
			Avicennia marina	8–28	5.3–13.5	14.9–248	4
			Heritiera littoralis	5–22.5	4.9–9.5	3.9–121.2	3

[a] Above-ground biomass is given in kg dry weight (kg DW) and includes stem, branch, leaf and prop root (in the case of *Rhizophora* sp.) components. An exception is the study by Lang'at (2008) where above-ground biomass comprises stem weight only. In the study by Kirui (2006) sample sizes for *Avicennia* sp. are the total number of stems (treated separately during analysis) and numbers in parentheses are the actual number of harvested trees. The study by Poungparn et al. (2002) included data sourced from other studies; see original paper for details.

[b] Plantation age at time of harvest in Kairo et al. (2009) was 5 years old for *R. mucronata* and *S. alba* and 8 years old for *C. tagal* and *A. marina*.

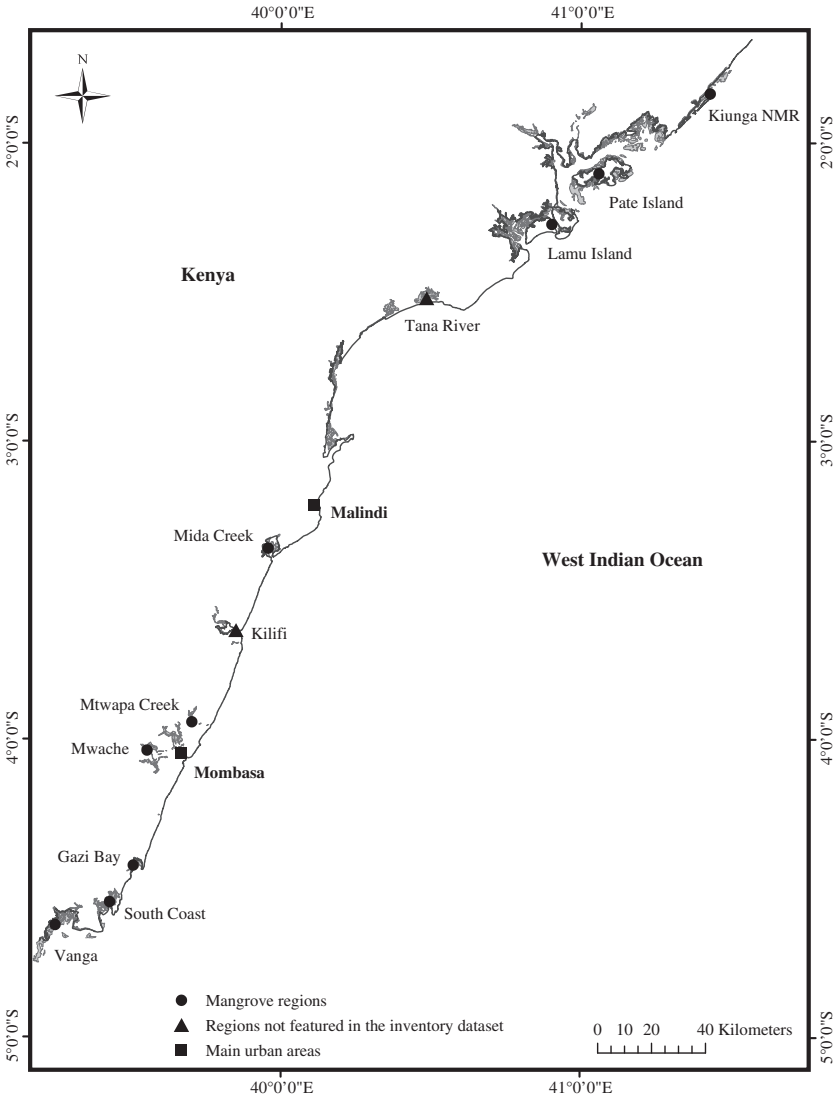

Fig. 1. Kenya coastline showing areas of mangrove forest where inventory data has been collected (dots). Inventory data collected within the general area of Lamu Island and Pate Island constitute the "South Lamu" study region. Kiunga NMR stands for Kiunga National Marine Reserve. Please note that the mangrove area defined as the "Tana River" region in this study spans the official districts of Kilifi and Tana River in Kenya and encompasses the mangroves just North of Malindi to the border of Lamu District. Kenya GIS base-map and mangrove shape-file obtained from the World Resources Institute (available at: <http://www.wri.org/>).

factor due to the unbalanced nature of the harvest dataset which has insufficient replication of species data at each site to allow separation of any possible variation in AGB attributable solely to either factor. In addition, Zianis and Mencuccini (2004) showed that within-species variability in allometric coefficients across sites is just as large as the variability in coefficients across species. Given that the harvest dataset comprises data from various studies any differences between the species_site groupings could also potentially incorporate an effect of study origin. However, harvest methodologies are broadly consistent across studies therefore it is likely the case that the random effects predictions are largely reflective of the differences across groups due to species and site effects.

Linear mixed-effects models were fitted using the lme4 package within R statistical software version 2.15.0 (Bates et al., (2011), http://CRAN.R-project.org/package=lme4). Prior to model fitting the logged predictive variables were centred at their mean to reduce any correlation between intercept and slope coefficients. Models were initially fitted using maximum likelihood (ML) estimation and compared using the Deviance Information Criterion (DIC) as outlined in Gelman and Hill (2007). In order to identify the best fixed and random effects terms for inclusion in the final model eight candidate models were fitted to the data (Table 2). Model notation follows that of Gelman and Hill (2007) where $\ln(y_i)$ is the response (AGB in this study) for the ith individual, α is the intercept, β represents the coefficients for the predictive variables diameter ($\ln(x_i)$) and height ($\ln(z_i)$) and σ_y^2 is the residual or the unexplained 'within-group' variance. The subscript term *j[i]* indexes the ith individual within the jth group and denotes where the intercept or a coefficient has been allowed to vary across groups ($j = 1, \ldots, J$) as a random effect.

Model I was the simplest model and included a random effects term for the intercept only whilst the slopes of both predictive variables were kept constant across groups (Table 2). The inclusion of a random effects term for $\ln(x_i)$ and $\ln(z_i)$ coefficients in models II and III respectively led to a reduction in the DIC value in comparison with model I. In order to ascertain if both diameter and height were needed as predictive variables within the model; models IV and V excluded each variable as a fixed effect (and hence as a random effect) in turn. As shown in Table 2 there is clearly a need to include both variables as fixed effects within the model. This is especially evident in the case of model V where exclusion of diameter from the model had a large impact on the DIC value. Models

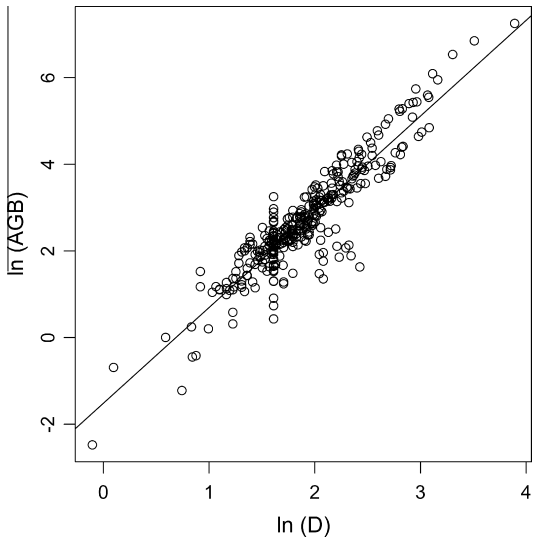

Fig. 2. Relationship between above-ground biomass (AGB) and stem diameter (D) of harvested mangrove trees after transformation by natural log. The vertical arrangement of data points at approximately $\ln(D) = 1.6$ is mostly due to data from the study by Kairo et al. (2009) which focused on harvesting trees from plantation forests of known age whereby a large proportion of data points arising from this study were of similar stem diameter (~5 cm).

Table 2
Comparison of candidate models fitted using maximum likelihood (ML) estimation, with corresponding DIC values.[a]

Model	DIC
I. $\ln(y_i) \sim N(\alpha_{j[i]} + \beta \ln(x_i) + \beta \ln(z_i), \sigma_y^2)$, for $i = 1,\ldots,n$,	274.1
II. $\ln(y_i) \sim N(\alpha_{j[i]} + \beta_{j[i]} \ln(x_i) + \beta \ln(z_i), \sigma_y^2)$, for $i = 1,\ldots,n$,	231.5
III. $\ln(y_i) \sim N(\alpha_{j[i]} + \beta \ln(x_i) + \beta_{j[i]} \ln(z_i), \sigma_y^2)$, for $i = 1,\ldots,n$,	220.3
IV. $\ln(y_i) \sim N(\alpha_{j[i]} + \beta_{j[i]} \ln(x_i), \sigma_y^2)$, for $i = 1,\ldots,n$,	260.5
V. $\ln(y_i) \sim N(\alpha_{j[i]} + \beta_{j[i]} \ln(z_i), \sigma_y^2)$, for $i = 1,\ldots,n$,	603.7
VI. $\ln(y_i) \sim N(\alpha_{j[i]} + \beta_{j[i]} \ln(x_i z_i), \sigma_y^2)$, for $i = 1,\ldots,n$,	299.1
VII. $\ln(y_i) \sim N(\alpha_{j[i]} + \beta_{j[i]} \ln(x_i^2 z_i), \sigma_y^2)$, for $i = 1,\ldots,n$,	240.1
VIII. $\ln(y_i) \sim N(\alpha_{j[i]} + \beta_{j[i]} \ln(x_i) + \beta_{j[i]} \ln(z_i), \sigma_y^2)$, for $i = 1,\ldots,n$,	206.1*

[a] The asterisk symbol denotes that model VIII was the best model overall.

were also fitted using two new combined predictive variables: $\ln(x_i z_i)$ and $\ln(x_i^2 z_i)$, both of which were logged and centred prior to model fitting as before. However, as shown in Table 2 models VI and VII using the combined variables displayed a poorer overall fit in comparison with models II and III (Table 2). Model VIII had the lowest DIC value of all the models under consideration indicating that the inclusion of a random effects term for the coefficients of both $\ln(x_i)$ and $\ln(z_i)$ was needed in order to account for variability in AGB across groups.

Model VIII was considered to be the most appropriate model overall and was subsequently re-fitted using restricted (or residual) maximum likelihood (REML) estimation in order to produce the best unbiased estimates of variance and co-variance parameters (Pinheiro and Bates, 2000). In model VIII the terms α_j, β_{jx} and β_{jz} signify that these parameters have themselves been modelled yielding a partial pooling estimate of α and the coefficients β_x and β_z for each group along with an estimate of the overall population mean and the 'between-group' variance (estimated from the data). The group-level model for model VIII can be written as:

$$\begin{pmatrix} \alpha_j \\ \beta_{jx} \\ \beta_{jz} \end{pmatrix} \sim N\left(\begin{pmatrix} \mu_\alpha \\ \mu_{\beta x} \\ \mu_{\beta z} \end{pmatrix}, \begin{pmatrix} \sigma_\alpha^2 & \rho_1 \sigma_\alpha \sigma_{\beta x} & \rho_2 \sigma_\alpha \sigma_{\beta z} \\ \rho_1 \sigma_\alpha \sigma_{\beta x} & \sigma_{\beta x}^2 & \rho_3 \sigma_{\beta x} \sigma_{\beta z} \\ \rho_2 \sigma_\alpha \sigma_{\beta z} & \rho_3 \sigma_{\beta x} \sigma_{\beta z} & \sigma_{\beta z}^2 \end{pmatrix} \right), \text{ for } j = 1,\ldots,J, \quad (3)$$

where the overall mean across all groups (the fixed effects estimates) for the intercept, slope of $\ln(x_i)$ and the slope of $\ln(z_i)$ are denoted by μ_α, $\mu_{\beta x}$ and $\mu_{\beta z}$ respectively. The between-group variance in the intercept, slope of $\ln(x_i)$ and the slope of $\ln(z_i)$ are given as σ_α^2 and $\sigma_{\beta x}^2$ and $\sigma_{\beta z}^2$ respectively. The parameters ρ_1, ρ_2 and ρ_3 are also estimated as the between-group correlations of the α's and β's (e.g. $\rho_1 \sigma_\alpha \sigma_{\beta x}$ is the correlation between the group intercepts and slopes of $\ln(x_i)$).

2.2.3. Simulation-based approach to biomass estimation

In order to estimate the biomass of mangroves along the entire Kenyan coastline the equations developed in this study were applied to a forest inventory dataset (detailed in Section 2.3) comprising 498 plots inventoried during the period 2007–2012. The modelling process described in Section 2.2.2 generated a mean biomass equation and a suite of specific equations; one for each of the eighteen species_site groups. The mean equation is comprised of the fixed effects estimates and can be regarded as a generic equation for Kenyan mangroves. The group specific equations represent the group departures from the fixed effects estimates (fixed effect estimates ± the group specific random effects) and are only valid for the specific groupings from which they were originally derived. Eight of the group specific equations can potentially be applied to the forest inventory dataset to estimate biomass as the remaining ten equations are only valid for species_site combinations occurring outwith Kenya. Therefore, group specific equations were applied to estimate the biomass of individual trees within the inventory dataset if those trees fell into one of the pre-existing groups identified within the harvest dataset. For example the group specific equation for Rhiz_Kin was applied to inventoried *Rhizophora* trees at Kinondo and so forth. In cases where inventoried trees did not fall into one of the pre-existing groups their biomass was estimated using the generic equation. The simulation-based approach adopted in this study allows for the propagation of measurement, parameter and residual uncertainty to estimates of biomass at the individual tree, plot and regional level.

2.2.4. Simulations for individual tree biomass

The above-ground biomass of each tree in the inventory dataset was simulated 10,000 times using a new set of simulated values for each iteration. In order to propagate measurement uncertainty possible values of stem diameter $\ln(D_{sim})$ and height $\ln(H_{sim})$ for each tree were randomly sampled from a normal distribution with mean equal to the observed value and one standard deviation conservatively assumed to be 5% and 10% of the observed diameter and height respectively. These assumed values of measurement uncertainty are consistent with the findings of previous studies (Chave et al., 2004; Gregoire et al., 1990; Phillips et al., 2000).

To propagate parameter uncertainty, possible values of the fixed effects intercept (α_{fixsim}) and coefficients for stem diameter ($\beta_{xfixsim}$) and height ($\beta_{zfixsim}$) were sampled from a multivariate normal distribution around means equal to μ_α, $\mu_{\beta x}$ and $\mu_{\beta z}$ from model VIII using the variance-covariance matrix of the fixed effects. In cases where the generic equation was applicable (to estimate the biomass of new trees in new groups) simulated values of the random effects for the intercept (α_{ransim}) and the coefficients for stem diameter ($\beta_{xransim}$) and height ($\beta_{zransim}$) were generated by sampling from a multivariate normal distribution around means equal to zero using the variance-covariance matrix of the group level (or mean) random effects (Eq. (3)). In cases where a group specific equation was applicable (to estimate the biomass of new trees in existing groups) possible values of the random effects were simulated as for the generic equation, however values were sampled around means equal to the group specific random effects for the intercept and coefficients and used the variance-covariance matrix

of the group specific random effects. Simulated values were then used in Eq. (4) to calculate AGB biomass ($\ln(AGB_{pred})$) for each tree:

$$\ln(AGB_{pred}) = \alpha_{sim} + ((\beta_{xfixsim} + \beta_{xransim})\ln(D_{sim})) + ((\beta_{zfixsim} + \beta_{zransim})\ln(H_{sim})) \quad (4)$$

where α_{sim} is the un-centred intercept (calculated as shown in Eq. (5)) and corrects for the use of mean centred predictive variables diameter and height during model development (Section 2.2.2).

$$\alpha_{sim} = (\alpha_{fixsim} + \alpha_{ransim}) - ((\beta_{xfixsim} + \beta_{xransim})\bar{x}) - ((\beta_{zfixsim} + \beta_{zransim})\bar{z}) \quad (5)$$

where $\bar{x}$ and $\bar{z}$ are the mean logged values of diameter and height respectively from the harvest dataset. In order to account for residual uncertainty in biomass estimates; possible values of biomass ($\ln(AGB_{Est})$) were randomly sampled from a normal distribution with mean equal to $\ln(AGB_{pred})$ and standard deviation equal to σ_y (the standard deviation of σ_y^2) from model VIII. Values of $\ln(AGB_{Est})$ were then back-transformed by taking the exponent; producing 10,000 estimates of AGB (in kg DW) for each tree. The estimates for all trees within a plot were then summed at each iteration point yielding a distribution of 10,000 possible estimates of total biomass for each plot. The median was taken as the plot level biomass estimate as this provided the most typical value from skewed distributions of the simulations. The quantiles from the distribution of plot estimates were used for calculating the 95% prediction interval (95% PI) at the plot level.

2.2.5. Calculation of regional level prediction intervals

In order to upscale biomass estimates from plot to regional level, plots were first grouped according to the mangrove regions identified in the inventory dataset (Table 3). Plots within Lamu District were further sub-divided into those within Kiunga National Marine Reserve (NMR) and those outwith the reserve (hereafter "South Lamu"). Due to their close geographical proximity plots from Shirazi, Ramisi, Funzi and Bodo were aggregated to form the region "South Coast". The mean biomass estimate was calculated for each iteration (across all plots within a region) yielding a distribution of 10,000 possible mean biomass estimates. The mean of this distribution was taken as the regional level biomass estimate (Mg ha^{-1}) and provides the expected value of AGB taking into account the whole scale of values present in a specific geographical area. The quantiles from the distribution were used to calculate the 95% PI at the regional level.

2.2.6. Model validation

The predictive performance of model VIII was evaluated using a harvest dataset from the Zambezi Delta, Mozambique (Table 1). The simulation process detailed in Section 2.2.4 was repeated for the 23 trees in the Zambezi dataset. For each tree the median fitted value of AGB (kg) was obtained along with the 95% PI for the median.

2.3. Forest inventory dataset

A summary of the forest inventory dataset is provided in Table 3, recent estimates of mangrove cover by region are provided in Table 4 and the location along the Kenyan coastline of each region is shown in Fig. 1. The cover estimates in Table 4 were derived from 2.5 m resolution SPOT remote sensing imagery acquired over the Kenyan coastline during 2009–2011 (see Rideout et al., 2013 for further details). The inventory dataset is a combination of data collected by this and other studies. All studies conducted prior to 2010/2011 had the objectives of characterising and investigating mangrove structural variability and change in the southern coastal region. However, in the current study sampling strategy was tailored (as much as was practicable) towards facilitating both a statistical and remote sensing based approach to biomass estimation along the entire coastline. Thus studies within the inventory dataset differ in terms of sampling strategy and plot size. There is also an obvious bias in total sampling effort towards sites in the south coast (Table 3).

In general all inventory studies followed a standardised methodology of within-plot data collection. In all studies the species, stem diameter and total height of all trees within each plot which met the diameter measurement threshold were recorded. Stem diameter was recorded to the nearest millimetre and was measured at 1.3 m aboveground (DBH) except in the case of *Rhizophora* sp. where stem diameter was measured at ~30 cm above the highest prop root if this occurred above 1.3 m. In cases where trees branched below 1.3 m (common in *Avicennia* sp.) and branches met the diameter measurement threshold; the diameter and height of each branch was recorded separately. In the current study total tree height was measured using an ultrasonic vertex hypsometer (Haglöf, Sweden). In all other studies tree height was measured using a graduated pole.

2.3.1. Mida Creek and Lamu District

Forest inventory data from the Mida Creek area and Lamu District was collected as part of this study during June–August 2010 and 2011. Mida Creek (3°20′S, 40°00′E) is situated mid-way along the Kenyan coast ~23 km south of the town Malindi in Kilifi District. Some of the mangrove forest in this area falls within the boundaries of Watamu Marine National Park (WNMP); however the majority is outwith the protected area. Regardless of location (within or outside of WNMP) harvesting of mangroves is currently prohibited in the Mida Creek area. In total 14 plots within the Mida Creek area were inventoried comprising nine 0.04 ha (20 × 20 m) plots, four 0.25 ha (50 × 50 m) plots and one 0.5 ha (100 × 50 m) plot. None of the inventoried plots were located within the marine park.

The Lamu archipelago extends between 2°22′S, 40°48′E in the South and 1°44′S, 41°30′E in the North and is part of Lamu District. Lamu District currently holds the greatest proportion of remaining mangrove cover in Kenya (Table 4). Mangroves in the extreme north, close to the border with Somalia are part of Kiunga NMR and are considered to be the only remaining examples of relatively "pristine" mangrove forest in Kenya. Forty-one plots within Lamu District were inventoried comprising twenty-five 0.04 ha plots, fifteen 0.25 ha plots and one 0.5 ha plot. Within Lamu District sites visited included: Kiunga NMR ($n = 16$ plots), Pate Island area ($n = 15$) and Lamu Island area ($n = 10$).

Plots inventoried in Mida Creek ($n = 6$) and Lamu District ($n = 8$) during 2010 were all 0.04 ha in size. Plots were positioned at random within *Rhizophora* zones and all trees within each plot with stem diameter $\geqslant$2.5 cm were measured. Plots inventoried during 2011 were a mixture of 0.04 ha plots (Mida Creek: $n = 3$, Lamu District: $n = 17$) located at random within randomly chosen map grid squares (grid resolutions of 500 × 500 metres and 1000 × 1000 m) and larger plots (0.25 ha and 0.5 ha) which were positioned at random within larger areas pre-identified using optical and radar remote sensing imagery. These pre-identified areas were judged to be potentially distinct from each other in terms of forest structure/biomass and also to broadly represent the main levels of structural variation within the study region as a whole. This more targeted plot location strategy was for the purpose of facilitating future remote sensing work. All plots inventoried in 2011 included all trees within each plot which met the criteria of having stem diameter $\geqslant$5 cm.

2.3.2. Gazi Bay

The Gazi Bay inventory consists of 116 plots in total. As part of this study twenty-four 0.01 ha (10 × 10 m) plots were inventoried

Table 3
Provenance and summary of mangrove forest inventory dataset.[a]

Region	Study	Date	No. of plots	Plot size (ha)	Stem diameter range (cm)	Height range (m)
Mida Creek	This study	2010/2011	14	Variable (ranging from 0.01 - 0.5)	2.5–58	1.5–17.7
Lamu District:	This study	2010/2011				
South Lamu			25		2.4–54	1.8–28.5
Kiunga			16		2–49.8	1.3–23.7
Gazi Bay	This study	2010/2011	28		5–64	1.8–20.2
	CAMARV	2009	18	0.01	0.5–51	0.6–15
	UNDP	2009	70	0.01	2.2–63.3	2–21
Mtwapa Creek	Okello (unpublished results)	2010	54	0.01	2.5–46.9	0.5–15
Mwache	Kaino (2013)	2011	67	0.01	2–53	1–15
South Coast:	KMFRI	2007				
Shirazi			43	0.01	5–47.5	2–16
Ramisi			22	0.01	5–48.4	2.5–15
Funzi			24	0.01	5–43.2	1.5–15
Bodo			34	0.01	5–60.5	2–14
Vanga	KMFRI	2012	83	Variable (ranging from 0.0025 - 0.04)	2.5–72.5	1–25

[a] Study abbreviations are as follows; United Nations Development Programme (UNDP); Capacity Building for Mangrove Assessment, Restoration and Validation (CAMARV) and Kenya Marine and Fisheries Research Institute (KMFRI).

Table 4
Mangrove cover estimates for inventory regions derived from high-resolution SPOT satellite imagery.[a]

Region	Mangrove cover estimate (ha)	Proportion of total cover (%)
Mida Creek	1657.8	3.6
South Lamu	26609.1	57.1
Kiunga (NMR)	4763.8	10.2
Gazi Bay	589	1.3
Mwache	2667.1	5.7
Mtwapa Creek	519.4	1.1
South Coast	2253.1	4.8
Vanga	3440	7.4
Kilifi*	640.2	1.4
Tana river*	3433	7.4
Total cover	46572.5	

[a] Regions marked with asterisks' do not feature in the forest inventory dataset. For details of SPOT image processing and analysis see Rideout et al. (2013).

during July 2010 and four 0.25 ha plots were inventoried during August 2011. The smaller plots inventoried in 2010 were positioned randomly within the main identifiable mangrove zones and included all trees DBH $\geqslant$ 5 cm. The larger plots collected in 2011 were positioned using the same procedure as detailed above for the large plots in Section 2.3.1 and included all trees within each plot stem diameter $\geqslant$5 cm.

The remaining plot data (n = 88) from the Gazi Bay area were collected in 2009 as part of two internationally funded short-term projects. Eighteen 0.01 ha plots were inventoried in the area adjacent to Gazi village as part of a project entitled CAMARV (Capacity Building for Mangrove Assessment, Restoration and Valuation in East Africa) funded by the Natural Environment Research Council (NERC) of the United Kingdom. Seventy 0.01 ha plots were inventoried as part of a UNDP-GEF Small Grants Programme project co-ordinated by Gazi Womens Group. In both projects plots were randomly positioned along a transect within each identifiable mangrove zone and all trees within each plot were included in the inventory.

2.3.3. Mwache and Mtwapa Creek

Mwache (4°2′S, 39°33′E) and Mtwapa Creek (3°57′S, 39°43′E) are both examples of peri-urban mangroves due to their close proximity to the city of Mombasa and the town of Mtwapa respectively. Both areas are considered to be degraded due to a combination of sewage pollution, timber over-exploitation and in the case of Mwache; the heavy sedimentation and flooding associated with the *El Niño* event of 1997–1998 (Kitheka et al., 2002). Inventory data from Mtwapa Creek (n = 54) was collected in 2010 as part of a study by Okello (unpublished results). Data from Mwache (n = 67) was collected in 2011 as part of a study conducted by Kaino (2013) and funded by the Western Indian Ocean Marine Science Association (WIOMSA). Both studies used plot sizes of 0.01 ha. Plots at Mtwapa Creek were positioned along transects running perpendicular to the shoreline at ~50 m intervals and all trees with stem diameter $\geqslant$2.5 cm were measured. At the Mwache site plots were positioned along transects running perpendicular to the shoreline at 100 m intervals using a stratified sampling scheme based on observed differences in forest composition and structure. All trees with stem diameter $\geqslant$2 cm within each plot were measured.

2.3.4. South Coast

Forest inventory data from the South Coast (Shirazi, Ramisi, Funzi and Bodo) was collected in 2007 by KMFRI as part of a Kenya government funded project. In total there are data from one hundred and twenty-three 0.01 ha plots comprising; Shirazi (n = 43), Ramisi (n = 22), Funzi (n = 24) and Bodo (n = 34). Plots were positioned at ~20 m intervals along transects running perpendicular to the shoreline and all trees with stem diameter $\geqslant$5 cm were included in the inventory.

2.3.5. Vanga

Mangroves close to the Kenya–Tanzania border were inventoried by KMFRI during January 2012. Plots inventoried within the Vanga mangrove system number 83 in total and are of variable size (sixty-nine 0.01 ha, six 0.04 ha and eight 0.0025 ha (5 × 5 m) plots). Plots were positioned within each identifiable mangrove zone using a stratified random sampling strategy and all trees $\geqslant$2.5 cm in diameter were recorded.

3. Results

3.1. Model VIII summary and key features

Overall, there is good correspondence between the fitted values of AGB (as estimated from model VIII) and the original observed values of AGB for trees in the harvest dataset (Fig. 3(a) and (b)). The mean absolute error (MAE) in predictions of AGB from model

VIII is 6.3 kg and the mean bias (observed-fitted) in predictions is an underestimate of just 0.06 kg. The model performs well at values of observed AGB $\leqslant$ 50 kg (Fig. 3(b)) which comprise 85% of the total dataset. There is some divergence from the reference line for the few trees in the harvest dataset with higher AGB values (Fig. 3(a)). Poorer model fit at higher AGB is likely due to the paucity of harvest data from larger trees with just 11 out of 337 trees in the dataset having an observed AGB $\geqslant$ 200 kg. Further diagnostic plots (data not shown) revealed no systematic trend in model residuals when plotted against the fitted values and against each of the predictive variables.

Mixed-effects models partition the total variance in the response variable (AGB in this study) between the main components of the model (Fig. 4). The proportional contribution of the random effects terms (σ^2_α, $\sigma^2_{\beta x}$, $\sigma^2_{\beta z}$) and the residual variance (σ^2_y) to the total variance was calculated for each term as:

$$\% \text{ contribution} = ((\sigma^2_\alpha/\text{tot\_var})100) \quad (6)$$

where e.g. σ^2_α is the variance in the model attributed to between-group differences in the intercept and tot_var is the total variance from model VIII calculated as the variance of the logged values of total above-ground biomass of the 337 trees in the harvest dataset. Thus, the contribution to the total variance attributable to the combined fixed effects terms was calculated as:

$$\% \text{ contribution} = (((\text{tot\_var} - (\text{sum}(\sigma^2_\alpha + \sigma^2_{\beta x} + \sigma^2_{\beta z} + \sigma^2_y)))/\text{tot\_var})100) \quad (7)$$

As expected, most of the variability in AGB was accounted for in model VIII by the fixed effects terms (Fig. 4). Together the random effects terms accounted for 41% of the variance in AGB. Between-group variability in the slopes of the predictive variables diameter and height was very similar accounting for 18% and 19% of the total variance respectively. In combination the fixed and random effects explained 94% of the variability in AGB leaving a relatively small residual variance of 6% (Fig. 4).

The random effects represent the group-specific departures (either ±) from the fixed effects estimate of the intercept and the coefficients for diameter and height. There is clearly some between-group variability in the random effects for the eight species_site groups occurring in Kenya (Fig. 5). The 95% PI around the random effects is more constrained for groups with a larger sample size (Fig. 5) and there is some degree of overlap in the prediction intervals between most groups.

The random effects for most groups fall within the bounds of the 95% confidence interval (95% CI) of the fixed effects estimate of each parameter (Fig. 5). However, the predicted random effect for the intercept of group Rhiz_Gaz and the coefficient of height for group Avic_Gaz show no overlap with the fixed effects estimates for these parameters. For group Sonn_Gaz there is a pronounced departure from both the fixed effects estimates and from the predicted random effects for the other groups. Such deviation from the fixed effects estimates suggest that the allometry for these species_site groupings may be distinct from that of the other groups in the harvest dataset and highlights the general need for the inclusion of group effects in regression models.

3.2. Model validation

For harvested trees in the Zambezi Delta predictions of median AGB (±95% PIs) from model VIII correspond well with the original observed values of AGB (Fig. 6). A linear regression between the logged observed values and predicted median values of AGB was used to further assess the predictive ability of model VIII ($R^2 = 0.96$, $p = < 0.001$). The 95% confidence interval for the intercept includes zero (−0.23 ± 0.37) and for the regression slope includes one (1.01 ± 0.09). The uncertainty around predictions is well constrained for trees with lower AGB but increases with increasing predicted AGB.

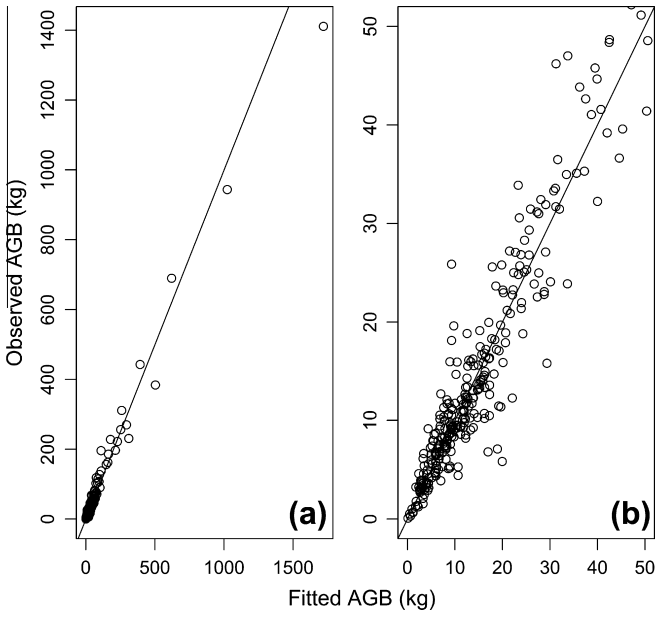

Fig. 3. (a) Total above-ground biomass (AGB) in kg as measured for each tree in the harvest dataset versus the corresponding fitted value (kg) from model VIII and (b) as (a) but re-scaled to show in detail the correspondence between observed and fitted values at the lower range of AGB. The reference lines shown in (a) and (b) represent a 1:1 correspondence between observed and fitted values.

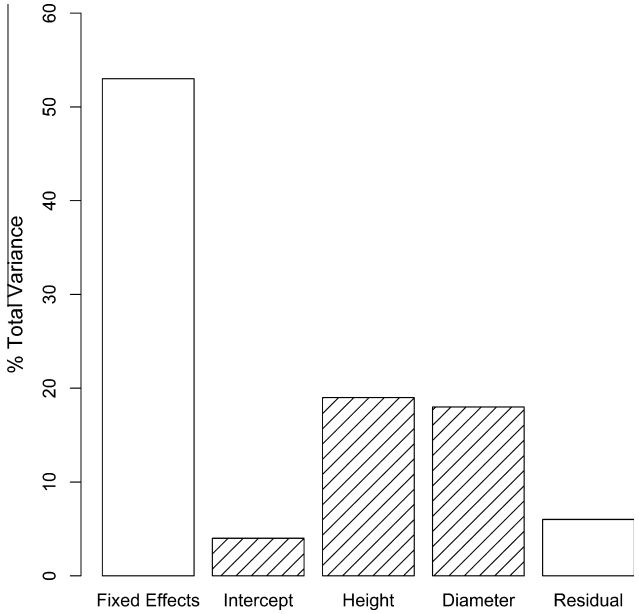

Fig. 4. Proportion of the total variability in AGB of harvested trees associated with the fixed effects terms, the random effects terms (hatched bars) and the remaining unexplained (residual) variance from Model VIII.

3.3. Plot level AGB estimates

Plot level estimates of mangrove AGB vary greatly within and between regions (Fig. 7). Within each study region (except Kiunga) there are two orders of magnitude difference between the smallest and largest plot estimates. If the 95% PIs are considered then the scale of maximum AGB across regions ranges between

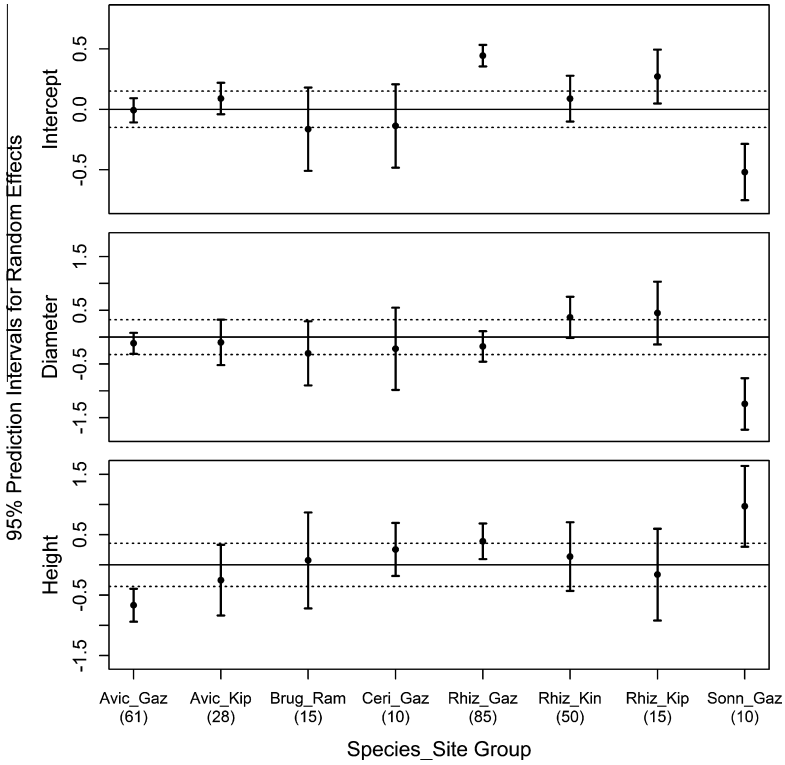

Fig. 5. Group-specific random effects (±95% PI) for the intercept and the coefficients of diameter and height. The solid line at zero represents no departure from the fixed effects estimate for each parameter and the dashed lines on either side are the upper and lower limits of the 95% CI of the fixed effects estimate. Species_site groups correspond to the first four letters of the species followed by the first three letters of the site (see Table 1). Numbers in parentheses denote sample size for each group.

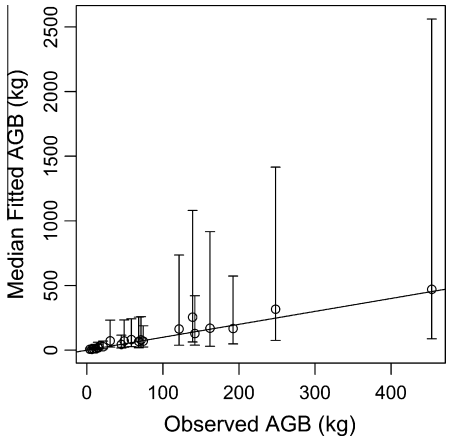

Fig. 6. Total above-ground biomass (AGB) in kg as measured for each tree in the Zambezi harvest dataset versus the corresponding median fitted value (kg ±95% PI) from model VIII. The 95% PI is the difference between the 97.5% and 2.5% quantiles of the simulated distribution of possible values of median AGB for each tree. The reference line represents a 1:1 correspondence between observed and fitted values.

~200 Mg ha^{-1} at Mida Creek to >2000 Mg ha^{-1} at Vanga. For each region the uncertainty in estimates is tightly constrained for plots with low values of AGB but there appears to be a general pattern of larger prediction intervals around estimates for plots with higher AGB (Fig. 7). For some regions there is considerable variation in the PIs of plots with similar median AGB estimates (e.g. see Mwache plots 45 and 46 in Fig. 7). It is likely that larger PIs around the estimates of some plots is not associated with higher biomass *per se* but is due to the presence of large diameter trees in these plots for which the biomass has been estimated with relatively less precision.

3.4. Regional level AGB estimates

As expected, estimates of mean AGB vary amongst the study regions which span the entire Kenyan coastline (Fig. 8). There is a difference of >120 Mg ha^{-1} between the lowest estimate for mangroves at Mtwapa Creek near Mombasa (73 Mg ha^{-1}) to the highest for mangroves within Kiunga NMR (200 Mg ha^{-1}). However, there is a general overlap between the prediction intervals of most regions and the estimates of mean AGB do not differ substantially between the regions Mwache, Gazi, South Coast, Vanga and South Lamu. Uncertainty around the estimates of mean AGB is reasonably well constrained with an absolute difference between upper and lower prediction limits of <50 Mg ha^{-1} for all regions.

The regional level estimates of mean AGB (Fig. 8) and mangrove cover (Table 4) were used in a basic up-scaling exercise in order to give an indication of the total AGB of mangroves within each region and within Kenya as a whole (Table 5). Up-scaled values of total mangrove AGB in megatonnes (Mt) were calculated by multiplying the regional level estimates of mean AGB (Mg ha^{-1}) shown in Fig. 8 by the corresponding estimate of total mangrove cover (ha) for each region (Table 4). There was no inventory data available for mangroves at Kilifi and Tana River therefore it was not possible to estimate mean AGB for these regions. For the purposes of up-scaling it was assumed that the mean AGB of mangroves at Kilifi and Tana River lies somewhere between that of Mtwapa Creek (the lowest regional mean) and Kiunga (the highest regional mean). Thus for sites Kilifi and Tana River two sets of possible values of total AGB ('Low' and 'High') were calculated using the lowest (Mtwapa Creek) and the highest (Kiunga) of the regional level estimates of mean AGB. Consequently there are also two sets of estimates of the total AGB of Kenyan mangroves; one in which the lowest estimates for Kilifi and Tana River were added to the total AGB of the other regions ('Kenya Low') and one in which the

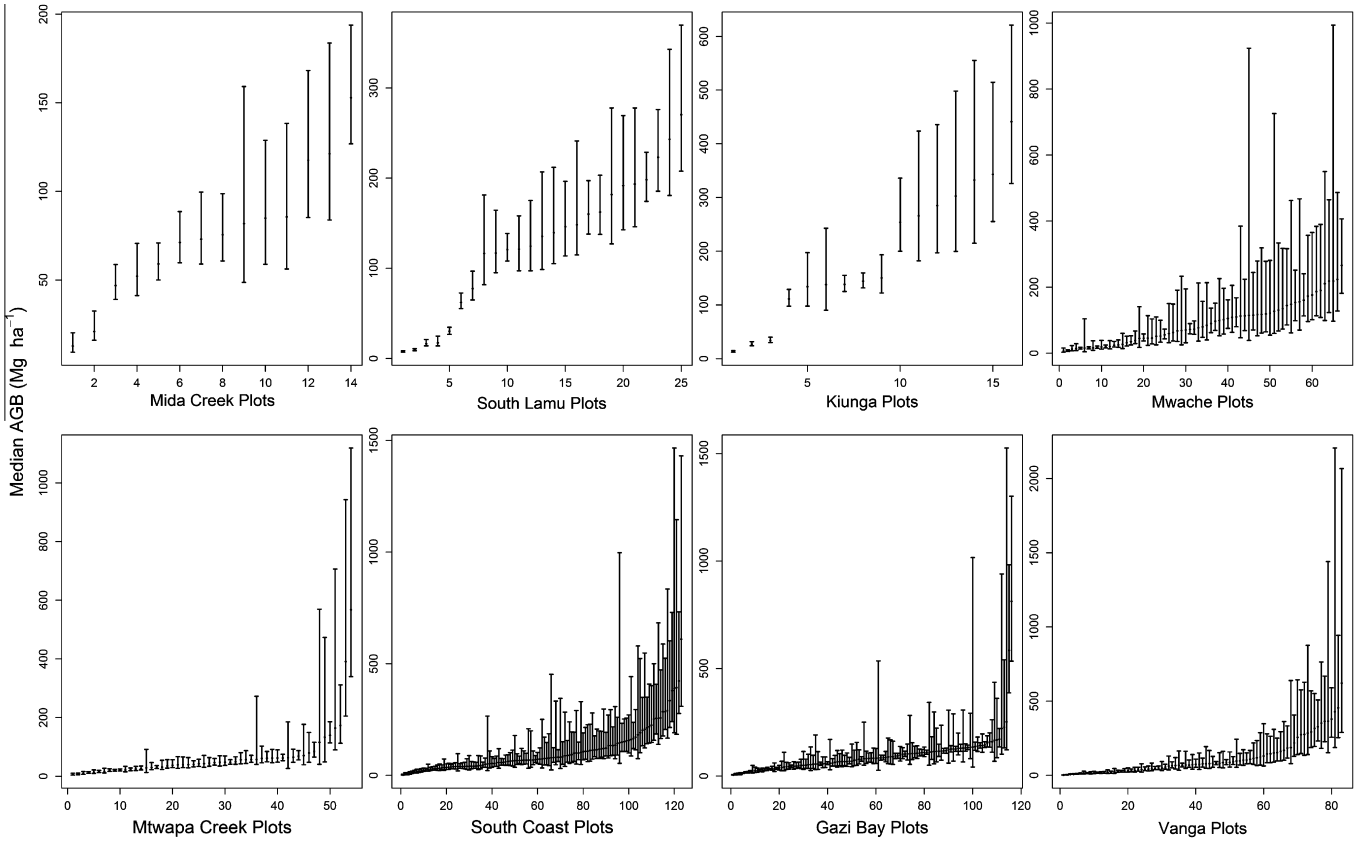

Fig. 7. Estimated median above-ground biomass (AGB) of each plot within the forest inventory dataset (±95% PI). Plots have been grouped according to the eight regions identified in the inventory dataset. For each region plots appear in ranked order from low to high estimated AGB. The 95% PI is the difference between the 97.5% and 2.5% quantiles of the simulated distributions of possible values of median AGB for each plot.

highest estimates were used ('Kenya High'). Lamu District (South Lamu + Kiunga) holds the highest proportion (~69–75% dependent on Kenya total) of mangrove AGB in Kenya (Table 5). Despite having one of the lowest estimates of mean AGB the estimated total AGB of mangroves at Mida Creek is more than double that of Gazi Bay due to the higher mangrove cover at Mida Creek.

The uncertainty around the estimates of total AGB are generally well constrained for all regions (Table 5). However, the Low and High estimates of total AGB for Kilifi and Tana River differ by a factor of ~2.7. This constitutes another level of uncertainty for these regions and consequently the overall total for Kenya which differs by ~8% between Low and High estimates.

4. Discussion

4.1. Applicability and interpretation of Model VIII

This study used mixed-effects modelling to account for both species and site variability in the allometric relationship for mangroves producing a generic equation for Kenyan mangroves and a set of species-site specific equations. The procedure for uncertainty propagation employed in the current study ensures that estimates of AGB at different spatial scales are accompanied by a realistic measure of the total uncertainty. It is important to note that although mangroves have been used as a case study here, the kind of models and methodologies presented can be regarded as broadly applicable to forests in general.

The practical application of the equations developed in the current study is dependent on the target of inference. The set of species-site specific equations are only applicable to four species within the Gazi Bay region and simulations using these equations account for the uncertainty in predicting the AGB of a new tree within a pre-existing group. In contrast, the generic equation has a much broader application as it can be used to predict the AGB of new trees where there is no pre-existing knowledge of the specific species-site allometric relationship: the most commonly encountered scenario in practical biomass studies. The generic equation offers a far better solution than simply disregarding the additional uncertainty involved in applying an equation that was perhaps derived for a different species and/or a different site.

The predictions of AGB from model VIII show good correspondence with the observed values of AGB used to fit the model (Fig. 3). Perhaps more importantly, the median fitted values of AGB (±95% PIs) from model VIII show good overall correspondence with the observed values of AGB for trees within the Mozambican validation dataset (Fig. 6). This would seem to indicate that accounting for variance due to species and site effects in biomass regression models is important if they are to be used effectively elsewhere to predict AGB. Indeed, a large proportion of the total variance in model VIII was attributed to between-group variability in the coefficients of the predictive variables diameter and height (Fig. 4). Both species and site specificity in the allometric relationship for mangroves is indicated by the group-specific random effects (Fig. 5). Most groups show some overlap in predicted random effects but there are some differences between species at the same site (species_Gaz groups) and between sites for the same species (Rhiz_site groups). However the use of a combined species_site grouping factor precludes any conclusion regarding the relative contribution of each factor (species and site) to the total variance in the allometric relationship. It is also not possible to formally assess the potential contribution of a study effect to the predicted random effects in this

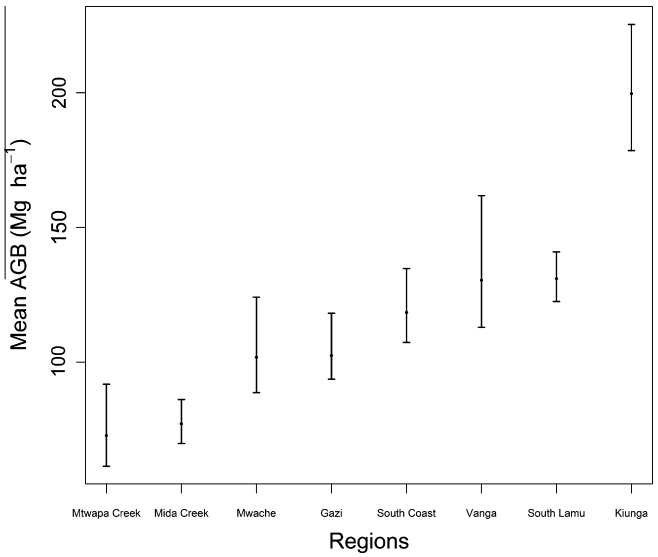

Fig. 8. Estimated mean AGB (±95% PI) of mangroves within each region. The 95% PI is the difference between the 97.5% and 2.5% quantiles of the simulated distribution of possible values of mean AGB for each region.

Table 5
Estimated total mangrove above-ground biomass (AGB) for Kenya and for each region within Kenya.[a]

Region	2.5% Quantile of total AGB (Mt)	Mean of total AGB (Mt)	97.5% Quantile of total AGB (Mt)
Mtwapa Creek	0.032	0.038	0.048
Mida Creek	0.116	0.128	0.143
Mwache	0.237	0.272	0.331
Gazi Bay	0.055	0.060	0.070
South Coast	0.242	0.267	0.304
Vanga	0.388	0.449	0.556
South Lamu	3.260	3.486	3.749
Kiunga	0.851	0.951	1.073
Kilifi (Low)	0.039	0.047	0.059
Kilifi (High)	0.114	0.128	0.144
Tana River (Low)	0.211	0.250	0.315
Tana River (High)	0.613	0.685	0.774
Kenya Total (Low)	5.431	5.947	6.648
Kenya Total (High)	5.908	6.464	7.192

[a] 1 Megatonne (Mt) = 1 million tonnes. The uncertainty around estimates of total AGB for each region is represented by the 2.5% and 97.5% quantiles of the mean.

study. However, as mentioned in Section 2.2.2 any such effect is assumed to be minimal due to the general agreement in methodology across studies included in the harvest dataset. The only study which differed notably in methodology was that of Lang'at (2008) where total above-ground biomass comprised stem weight only (Table 1). In this case the sample size was fairly small (15 trees) and re-fitting model VIII after excluding this dataset did not substantially alter the fixed effects estimates, predicted random effects or residual variance.

In modelling the covariance of the distribution of random effects, the constraints imposed by the mixed-effects model used in the current study on the estimated correlation parameters may be considered too restrictive when more than two coefficients vary by group (Gelman and Hill, 2007). Although outwith the scope of the current paper; an alternative approach for future study would be to use a scaled inverse-Wishart distribution as the prior for modelling the covariance matrix of the random effects in a fully Bayesian model (Dietze et al., 2008; Gelman and Hill, 2007).

Ideally regression models should not be applied outwith the data range for which they were derived (Chave et al., 2005; Chave et al., 2004). The lack of large tree harvest data means that extrapolation is often a practical necessity when estimates of AGB are needed for large trees within forest inventory datasets. In this study, it is assumed that the log-log linear relationship will hold for trees beyond the original data range. It is, however, acknowledged that this may not be the case and that the estimates of AGB for trees outwith the data range recorded in harvest dataset will include additional uncertainty due to extrapolation. Only a very small proportion of trees in the inventory dataset (0.1%) had a recorded diameter exceeding that found within the harvest dataset and none exceeded the height range. However, the effect of having limited information regarding the allometric relationship for large trees is apparent in the poorer model fit at higher AGB values (Fig. 3). It is also apparent (to some degree) in the width of the prediction intervals around the larger trees in the validation dataset and the estimates of AGB at the plot, regional and landscape level. This is presumably due to the fact that by accounting for the covariance of the predictive uncertainty at the single tree level in producing estimates of AGB at aggregated levels (e.g. a plot) the aggregated predictive uncertainty is realistically larger than if the AGB of multiple trees had simply been summed (Wutzler et al., 2008). In addition, the greater width of the PIs for larger trees is an inevitable consequence of using a log-normal model where the variability is related to the mean on the linear scale. An approach to consider for future study would be to investigate the use of alternative distributions for the variability.

The 95% PIs in the current study are generally well constrained given that measurement and predictive uncertainty have been fully propagated to estimates. In addition, prediction intervals take into account both the uncertainty in estimating the conditional mean of the response and the variability in the conditional distribution of the response and as such are generally larger than the frequentist confidence intervals employed to represent uncertainty in most other studies. However, for a few of the plots in the inventory dataset the upper limit of the PI around the median estimate of AGB is exceptionally high (Fig. 7) and exceeds the highest levels of AGB previously reported for mangroves. The effects of both extrapolation and small plot size could possibly explain these extreme upper PI values for selected plots. All of the affected plots measure just 10 $\times$ 10 m and contain two or more large diameter trees which in some cases exceed the maximum diameter (48.9 cm) found in the harvest dataset. The presence of a few large trees in a small plot can skew results, however tree level and sampling uncertainties tend to be reduced in larger plots (Chave et al., 2004).

4.2. Comparison and interpretation of large-scale AGB estimates

Previous allometry/biomass studies conducted in Kenya have focused on the development and application of species-specific allometric equations to mangroves at a particular site. As a result existing published estimates of AGB for Kenyan mangroves are on a species by site basis and in many cases refer to monoculture plantation forest established at Gazi Bay (Kairo et al., 2009; Kairo et al., 2008; Tamooh et al., 2009). Estimates of AGB for natural mangrove forest in Kenya vary considerably between sites but also between studies conducted at the same site. Within the Mida Creek area Gang and Agatsiva (1992) estimated the AGB of *Rhizophora* forest as 11.8 Mg ha^{-1}. However, their estimate is based on the data from just one plot and there is no mention of how this estimate was derived (Gang and Agatsiva, 1992). For the same species at Gazi Bay Slim et al. (1996) and Kirui et al. (2006) produced substantially higher estimates of mean AGB at 249 Mg ha^{-1} (± s.d. 40.1) and 452.02 Mg ha^{-1} respectively. Similar to the study by

Gang and Agatsiva (1992) the estimate of AGB from Slim et al. (1996) was based on the application of their allometric equation to *Rhizophora* trees within one 20 × 20 m mono-specific plot and therefore cannot reasonably be assumed to represent the variability of *Rhizophora* forest within Gazi Bay. The highest estimate from Kirui et al. (2006) is more akin to the level of AGB found in mangroves in South East Asia (Komiyama et al., 2008) and it is not clear how their mean estimate was derived. In contrast to previous studies, this study has focused on providing estimates of mangrove AGB at varying spatial scales. This different approach means that the estimates provided here are not readily comparable with those from previous biomass studies conducted in Kenya. However, to facilitate some kind of comparison the outputs of the simulation procedure (Section 2.2.4) were sub-set to provide an estimate of mean AGB for just *Rhizophora* forest at Gazi Bay of 134.5 Mg ha^{-1} (95% PI range 125.1–146.8 Mg ha^{-1}).

Estimates of biomass density (mean Mg ha^{-1}) at large spatial scales such as those produced in the current study can be regarded as a comparative tool by which to assess the level of AGB at different sites/regions or between countries or forest types. Levels of mean AGB have been found to vary considerably between mangrove forests across the globe (see review by Komiyama et al., 2008) ranging between 31.5 Mg ha^{-1} (± s.d. 2.9) for pioneer mangrove forest in French Guiana (Fromard et al., 1998) to 536.6 Mg ha^{-1} (95% CI range 327.6–743.5 Mg ha^{-1}) for mangroves in Micronesia (Donato et al., 2012). Such broad-scale variability can be attributed to differences in floristic composition, climatic conditions, hydrology, geomorphology, successional stage and disturbance history (Fromard et al., 1998).

The regional estimates of mean AGB (±95% PI) shown in Fig. 8. represent a best attempt at summarising the level of AGB within different mangrove regions in Kenya. The two regions with the lowest estimated mean AGB were Mtwapa Creek (72.8 Mg ha^{-1}, 95% PI range 61.4–91.9 Mg ha^{-1}) and Mida Creek (77.1 Mg ha^{-1}, 95% PI range 69.9–86.2 Mg ha^{-1}) and are comparable to the level of AGB (71–85 Mg ha^{-1}) found in mixed mangrove forests dominated by *R. mucronata* and *A. marina* in Sri Lanka (Amarasinghe and Balasubramaniam, 1992). The estimate for Mida Creek is somewhat lower than expected and could be due to insufficient inventory data from this region (n = 14 plots) but it is also likely reflective of the level of forest degradation in this area due to illegal and poorly managed logging practices (Kairo et al., 2002). The region with the highest estimate of mean AGB was Kiunga NMR (199.6 Mg ha^{-1}, 95% PI range 178.6–225.3 Mg ha^{-1}). This level of AGB is comparable to that reported for mangroves in Micronesia (Donato et al., 2012; Kauffman et al., 2011) and mature coastal mangroves in French Guiana (Fromard et al., 1998) and exceeds the estimate by Donato et al. (2011) of 169.9 Mg ha^{-1} for oceanic mangroves in the Indo-Pacific region.

Although the estimates of AGB produced in this study are statistically robust, it is important to note the underlying assumption that estimates at large spatial scales have been obtained using a sample which is representative of the variability in forest composition and structure within the area in question (Chave et al., 2004). The estimates of mean AGB in this study were derived using all available current inventory data for each region. It seems reasonable to assume that due to the sampling strategy employed (stratified random) and the comparatively large sampling effort (total number of plots sampled) that the mangrove areas in the South of Kenya (Gazi Bay, Mwache, Mtwapa Creek, South Coast and Vanga) have been adequately sampled. In addition, the large within-region variability in estimates of median AGB at the plot level (Fig. 7) would suggest that there has been no sampling bias in terms of plot location, for example by preferentially locating plots in areas likely to yield high biomass and that the range of possible biomass values within each region has been adequately captured.

The regional estimates for Mida Creek and Lamu District (South Lamu and Kiunga) are based on relatively small inventory datasets (n = 14 plots in Mida Creek, 25 in South Lamu and 16 in Kiunga) due to the larger resource requirement and practical difficulties (e.g. accessibility) associated with sampling areas in the North. While the sampling strategies employed in these regions (random and stratified random) are appropriate from a statistical point of view; it is recommended that further data collection is undertaken in order to increase sample size and ensure representivity in these regions. This is particularly important in the case of Lamu District which covers a large geographical area and is worthy of further division into smaller sub-regions. For example, the mangroves of Dodori Creek (Dodori National Reserve, Lamu District) were not sampled in the current study but should probably be considered as a distinct mangrove system.

In considering the regional and Kenya-wide estimates of total AGB provided in Table 5 it is acknowledged that: (1) the estimates of mean AGB (±95% PIs) used in up-scaling are assumed to be regionally representative as discussed above and (2) the uncertainty associated with the estimates of mangrove cover derived from the remote sensing data has not been accounted for. Bearing in mind these caveats the estimates (±95% PIs) shown in Table 5 can still be viewed as a useful comparative overview of the level of total AGB stocks currently held within each region. There is undoubtedly scope for large-scale estimates to be further refined in the future. In particular there is a need for current inventory data to be collected within the regions Kilifi and Tana River (as defined in this study) not only to constrain the regional estimates but also the Kenya-wide estimate of total AGB. In addition, if and when future remote sensing work allows for the detailed mapping of mangrove cover and structural characteristics in each region it may become possible (and desirable) to produce large-scale estimates of AGB based on up-scaling by forest strata.

The stratification of forest cover is recommended for the reporting of forest carbon pools (IPCC, 2006) and there are a variety of stratification options still under consideration for future REDD reporting (Maniatis and Mollicone, 2010). Mangroves are generally considered to display species zonation and have traditionally been stratified by such 'zones' (Hogarth, 1999). However, not all mangroves display well-defined patterns of zonation (e.g. Mida Creek) and other options for stratification for example based on structural characteristics may be more appropriate in some situations. Various remote sensing techniques have been used in recent years to map mangroves at fine to large spatial scales (see review by Kuenzer et al., 2011). Such techniques offer the potential for fast and repeatable estimates of cover, and in the case of radar remote sensing above-ground biomass to be made based on mangrove structural parameters (Fatoyinbo et al., 2008; Held et al., 2003; Lucas et al., 2007).

It is anticipated that if required and pending any further collection of new harvest data, the model and methodology for uncertainty propagation presented in the current study could be used to produce estimates of mean AGB for use in future up-scaling exercises based on some stratification system with only minor modification to the existing procedures.

Acknowledgements

This research was funded by the Natural Environment Research Council (NERC), UK to which we are very grateful. We are also very grateful for the support provided by our collaborating partner Kenya Marine and Fisheries Research Institute (KMFRI) and additional support in the field provided by Kenya Forest Service (KFS). Many thanks to all those who provided the raw data used for model development and application and to WWF, Mozambique/KMFRI for providing us with a validation dataset. Data collection in

Mwache was supported by the WIOMSA-MASMA regional project on "Resilience of mangroves and dependent communities in the WIO region to climate change", Grant No: MASMA/CC/2010/08. Satellite imagery was provided by Spot Image through the Planet Action initiative as part of a larger project funded by the Ecosystem Services for Poverty Alleviation (ESPA) programme [under the Swahili Seas NE/I003401/1 project]. The ESPA programme is funded by the Department for International Development (DFID), the Economic and Social Research Council (ESRC) and the Natural Environment Research Council (NERC) of the UK. Additional SPOT imagery was provided under the European Space Agency (ESA) Category-1 scheme (Project ID: 8177). All processing of satellite imagery was carried out by Dr. Karin Viergever at ecometrica (Edinburgh, UK) and Neha Joshi to whom we are very grateful for lending their expertise. We wish to thank all those involved for their hard work in collecting the inventory data for the current study, in particular Mr Bernard Kivyatu. Many thanks to Mr Luke Smallman (University of Edinburgh, UK) for help with programming in R and to Dr Giles T. Innocent (Biomathematics and Statistics Scotland (BioSS)) for providing statistical advice. Finally, we wish to thank two anonymous reviewers for their comments and suggestions for improvement to the manuscript.

References

Aburto-Oropeza, O., Ezcurra, E., Danemann, G., Valdez, V., Murray, J., Sala, E., 2008. Mangroves in the Gulf of California increase fishery yields. PNAS 105, 10456–10459.

Akaike, H., 1987. Factor analysis and AIC. Psychometrika 52, 317–332.

Alongi, D.M., 2002. Present state and future of the world's mangrove forests. Environ. Conserv. 29, 331–349.

Amarasinghe, M.D., Balasubramaniam, S., 1992. Structural properties of two types of mangrove stands on the northwestern coast of Sri Lanka. Hydrobiologia 247, 17–27.

Bates, D., Maechler, M., Bolker, B., 2011. lme4: Linear mixed-effects models using S4 classes. R package version 0.999375-42. <http://CRAN.R-project.org/package=lme4>.

Bosire, J.O., Bandeira, S., Rafael, J., unpublished results. Coastal climate change mitigation and adaptation through REDD+ carbon programs in mangroves in Mozambique: pilot in the Zambezi Delta. Determination of carbon stocks through localized allometric equations component. WWF report.

Bouillon, S., Borges, A.V., Castaneda-Moya, E., Diele, K., Dittmar, T., Duke, N.C., Kristensen, E., Lee, S.Y., Marchand, C., Middelburg, J.J., Rivera-Monroy, V.H., Smith, T.J., Twilley, R.R., 2008. Mangrove production and carbon sinks: a revision of global budget estimates. Global Biogeochem. Cycles 22.

Brown, S., 2002. Measuring carbon in forests: current status and future challenges. Environ. Pollut. 116, 363–372.

Brown, S., Gillespie, A.J.R., Lugo, A.E., 1989. Biomass estimation methods for tropical forests with applications to forest inventory data. For. Sci. 35, 881–902.

Chave, J., Condit, R., Salomon, A., Hernandez, A., Lao, S., Perez, R., 2004. Error propagation and scaling for tropical forest biomass estimates. Philos. Trans. Roy. Soc. B 359, 409–420.

Chave, J., Andalo, C., Brown, S., Cairns, M.A., Chambers, J.Q., Eamus, D., Fölster, H., Fromard, F., Higuchi, N., Kira, T., Lescure, J.P., Nelson, B.W., Ogawa, H., Puig, H., Riéra, B., Yamakura, T., 2005. Tree allometry and improved estimation of carbon stocks and balance in tropical forests. Oecologia 145, 87–99.

Chmura, G.L., Anisfeld, S.C., Cahoon, D.R., Lynch, J.C., 2003. Global carbon sequestration in tidal, saline wetland soils. Global Biogeochem. Cycles 17.

Clough, B.F., Scott, K., 1989. Allometric relationships for estimating above-ground biomass in 6 mangrove species. For. Ecol. Manage. 27, 117–127.

Clough, B.F., Dixon, P., Dalhaus, O., 1997. Allometric relationships for estimating biomass in multi-stemmed mangrove trees. Aust. J. Bot. 45, 1023–1031.

Dahdouh-Guebas, F., Mathenge, C., Kairo, J.G., Koedam, N., 2000. Utilization of mangrove wood products around Mida Creek (Kenya) amongst subsistence and commercial users. Econ. Bot. 54, 513–527.

Dietze, M.C., Wolosin, M.S., Clark, J.S., 2008. Capturing diversity and interspecific variability in allometries: a hierarchical approach. For. Ecol. Manage. 256, 1939–1948.

Donato, D.C., Kauffman, J.B., Murdiyarso, D., Kurnianto, S., Stidham, M., Kanninen, M., 2011. Mangroves among the most carbon-rich forests in the tropics. Nat. Geosci. 4, 293–297.

Donato, D.C., Kauffman, J.B., Mackenzie, R.A., Ainsworth, A., Pfleeger, A.Z., 2012. Whole-island carbon stocks in the tropical Pacific: implications for mangrove conservation and upland restoration. J. Environ. Manage. 97, 89–96.

Duarte, C.M., Middelburg, J.J., Caraco, N., 2005. Major role of marine vegetation on the oceanic carbon cycle. Biogeosciences 2, 1–8.

Fatoyinbo, T.E., Simard, M., Washington-Allen, R.A., Shugart, H.H., 2008. Landscape-scale extent, height, biomass, and carbon estimation of Mozambique's mangrove forests with Landsat ETM+ and Shuttle Radar Topography Mission elevation data. J. Geophys. Res.-Biogeo. 113.

Fromard, F., Puig, H., Mougin, E., Marty, G., Betoulle, J.L., Cadamuro, L., 1998. Structure, above-ground biomass and dynamics of mangrove ecosystems: new data from French Guiana. Oecologia 115, 39–53.

Gang, P.O., Agatsiva, J.L., 1992. The current status of mangroves along the Kenyan coast – a case-study of Mida Creek mangroves based on remote-sensing. Hydrobiologia 247, 29–36.

Gelman, A., Hill, J., 2007. Data Analysis Using Regression and Multilevel/Hierarchical Models. Cambridge University Press, New York.

Gelman, A., Pardoe, I., 2006. Bayesian measures of explained variance and pooling in multilevel (hierarchical) models. Technometrics 48, 241–251.

Giri, C., Ochieng, E., Tieszen, L.L., Zhu, Z., Singh, A., Loveland, T., Masek, J., Duke, N., 2011. Status and distribution of mangrove forests of the world using earth observation satellite data. Global Ecol. Biogeogr. 20, 154–159.

Gregoire, T.G., Zedaker, S.M., Nicholas, N.S., 1990. Modeling relative error in stem basal area estimates. Can. J. For. Res. 20, 496–502.

Heath, L.S., Smith, J.E., 2000. An assessment of uncertainty in forest carbon budget projections. Environ. Sci. Policy 3, 73–82.

Held, A., Ticehurst, C., Lymburner, L., Williams, N., 2003. High resolution mapping of tropical mangrove ecosystems using hyperspectral and radar remote sensing. Int. J. Remote Sens. 24, 2739–2759.

Hogarth, P.J., 1999. The Biology of Mangroves. Oxford University Press, Oxford.

IPCC, 2006. Guidelines for National Greenhouse Gas Inventories. IGES, Japan.

Johnson, J.B., Omland, K.S., 2004. Model selection in ecology and evolution. Trends Ecol. Evol. 19, 101–108.

Kaino, J., 2013. Structure, biomass and cover change of a peri-urban mangrove forest in Kenya: a case study of Mwache Creek, Mombasa. MSc Thesis. Egerton University, Kenya.

Kairo, J.G., Dahdouh-Guebas, F., Gwada, P.O., Ochieng, C., Koedam, N., 2002. Regeneration status of mangrove forests in Mida Creek, Kenya: a compromised or secured future? Ambio 31, 562–568.

Kairo, J.G., Lang'at, J.K.S., Dahdouh-Guebas, F., Bosire, J., Karachi, M., 2008. Structural development and productivity of replanted mangrove plantations in Kenya. For. Ecol. Manage. 255, 2670–2677.

Kairo, J.G., Bosire, J., Langat, J., Kirui, B., Koedam, N., 2009. Allometry and biomass distribution in replanted mangrove plantations at Gazi Bay, Kenya. Aquat. Conserv.-Mar. Freshw. Ecosyst. 19, S63–S69.

Kathiresan, K., Bingham, B.L., 2001. Biology of mangroves and mangrove ecosystems. Adv. Mar. Biol. 40, 81–251.

Kauffman, J.B., Heider, C., Cole, T.G., Dwire, K.A., Donato, D.C., 2011. Ecosystem carbon stocks of Micronesian mangrove forests. Wetlands 31, 343–352.

Ketterings, Q.M., Coe, R., van Noordwijk, M., Ambagau, Y., Palm, C.A., 2001. Reducing uncertainty in the use of allometric biomass equations for predicting above-ground tree biomass in mixed secondary forests. For. Ecol. Manage. 146, 199–209.

Kirui, B., 2006. Allometric relations for estimating aboveground biomass of naturally growing mangroves, Avicennia marina FORSK (VIERH). and Rhizophora mucronata LAM. along the Kenya coast. MSc. Thesis. Egerton University, Kenya.

Kirui, B., Kairo, J.G., Karachi, M., 2006. Allometric equations for estimating above ground biomass of *Rhizophora mucronata* Lamk. (Rhizophoraceae) mangroves at Gazi Bay, Kenya. WIOJMS 5, 27–34.

Kirui, K.B., Kairo, J.G., Bosire, J., Viergever, K.M., Rudra, S., Huxham, M., Briers, R.A., 2012. Mapping of mangrove forest land cover change along the Kenya coastline using Landsat imagery. Ocean Coast. Manage. http://dx.doi.org/10.1016/j.ocecoaman.2011.12.004.

Kitheka, J.U., Ongwenyi, G.S., Mavuti, K.M., 2002. Dynamics of suspended sediment exchange and transport in a degraded mangrove creek in Kenya. Ambio 31, 580–587.

Komiyama, A., Jintana, V., Sangtiean, T., Kato, S., 2002. A common allometric equation for predicting stem weight of mangroves growing in secondary forests. Ecol. Res. 17, 415–418.

Komiyama, A., Poungparn, S., Kato, S., 2005. Common allometric equations for estimating the tree weight of mangroves. J. Trop. Ecol. 21, 471–477.

Komiyama, A., Ong, J.E., Poungparn, S., 2008. Allometry, biomass, and productivity of mangrove forests: a review. Aquat. Bot. 89, 128–137.

Kuenzer, C., Bluemel, A., Gebhardt, S., Quoc, T.V., Dech, S., 2011. Remote sensing of mangrove ecosystems: a review. Remote Sensing 3, 878–928.

Lang'at, J.K.S., 2008. Assessment of forest structure, regeneration and biomass accumulation of replanted mangroves in Kenya. MSc. Thesis. Egerton University, Kenya.

Lucas, R.M., Mitchell, A.L., Rosenqvist, A., Proisy, C., Melius, A., Ticehurst, C., 2007. The potential of L-band SAR for quantifying mangrove characteristics and change: case studies from the tropics. Aquat. Conserv.-Mar. Freshw. Ecosyst. 17, 245–264.

Maniatis, D., Mollicone, D., 2010. Options for sampling and stratification for national forest inventories to implement REDD+ under the UNFCCC. Carbon Balance Manage. 5, 9.

McKee, K.L., Cahoon, D.R., Feller, I.C., 2007. Caribbean mangroves adjust to rising sea level through biotic controls on change in soil elevation. Global Ecol. Biogeogr. 16, 545–556.

Okello, J.A., unpublished results. Mangrove wood formation as a basis of sustainable wood production in its climate context: The effect of increased sediment accumulation. Ph.D Thesis. Vrije Universiteit, Belgium.

Parresol, B.R., 1999. Assessing tree and stand biomass: a review with examples and critical comparisons. For. Sci. 45, 573–593.

Pendleton, L., Donato, D.C., Murray, B.C., Crooks, S., Jenkins, W.A., Sifleet, S., Craft, C., Fourqurean, J.W., Kauffman, J.B., Marba, N., Megonigal, P., Pidgeon, E., Herr, D., Gordon, D., Baldera, A., 2012. Estimating global "Blue Carbon" emissions from conversion and degradation of vegetated coastal ecosystems. PLoS ONE 7.

Phillips, D.L., Brown, S.L., Schroeder, P.E., Birdsey, R.A., 2000. Toward error analysis of large-scale forest carbon budgets. Global Ecol. Biogeogr. 9, 305–313.

Pinheiro, J.C., Bates, D.M., 2000. Mixed-effects Models in S and S-PLUS. Springer-Verlag, New York.

Poungparn, S., Komiyama, A., Patanaponpaipoon, P., Jintana, V., Sangtiean, T., Tanapermpool, P., Piriyayota, S., Maknual, C., Kato, S., 2002. Site-independent allometric relationships for estimating above-ground weights of mangroves. TROPICS 12, 147–158.

Primavera, J.H., 2005. GLOBAL VOICES OF SCIENCE: mangroves, fishponds, and the quest for sustainability. Science 310, 57–59.

Rideout, A., Joshi, N., Viergever, K., Huxham, M., Briers, R.A., 2013. Making predictions of mangrove deforestation: a comparison of two methods in Kenya. Glob. Change Biol. http://dx.doi.org/10.1111/gcb.12176.

Ryan, C.M., 2009. Carbon cycling, fire and phenology in a tropical savanna woodland in Nhambita, Mozambique. Ph.D. Thesis. University of Edinburgh, Edinburgh, UK.

Siikamaki, J., Sanchirico, J.N., Jardine, S.L., 2012. Global economic potential for reducing carbon dioxide emissions from mangrove loss. PNAS 109, 14369–14374.

Slim, F.J., Gwada, P.M., Kodjo, M., Hemminga, M.A., 1996. Biomass and litterfall of *Ceriops tagal* and *Rhizophora mucronata* in the mangrove forest of Gazi Bay, Kenya. Mar. Freshwater Res. 47, 999–1007.

Soares, M.L.G., Schaeffer-Novelli, Y., 2005. Above-ground biomass of mangrove species. I. Analysis of models. Estuar. Coast. Shelf Sci. 65, 1–18.

Steele, F., 2008. Introduction to multilevel modelling concepts: module 5. University of Bristol Centre for Multilevel Modelling: [online] Learning Environment for Multilevel Methodology and Applications (LEMMA) <http://www.bristol.ac.uk/cmm/>.

Steinke, T.D., Ward, C.J., Rajh, A., 1995. Forest structure and biomass of mangroves in the Mgeni Estuary, South-Africa. Hydrobiologia 295, 159–166.

Tamooh, F., Kairo, J.G., Huxham, M., Kirui, B., Mencuccini, M., Karachi, M., 2009. Biomass accumulation in a rehabilitated mangrove forest at Gazi Bay. In: Hoorweg, J., Muthiga, N. (Eds.), African Studies Collection, vol. 20. African Studies Centre, Leiden, pp. 138–146.

Valiela, I., Bowen, J.L., York, J.K., 2001. Mangrove forests: one of the world's threatened major tropical environments. Bioscience 51, 807–815.

van der Werf, G.R., Morton, D.C., DeFries, R.S., Olivier, J.G.J., Kasibhatla, P.S., Jackson, R.B., Collatz, G.J., Randerson, J.T., 2009. CO_2 emissions from forest loss. Nat. Geosci. 2, 737–738.

Wickramasinghe, S., Borin, M., Kotagama, S.W., Cochard, R., Anceno, A.J., Shipin, O.V., 2009. Multi-functional pollution mitigation in a rehabilitated mangrove conservation area. Ecol. Eng. 35, 898–907.

World Resources Institute. Poverty and ecosystems: Kenya GIS. <http://www.wri.org/>.

Wutzler, T., Wirth, C., Schumacher, J., 2008. Generic biomass functions for Common beech (*Fagus sylvatica*) in Central Europe: predictions and components of uncertainty. Can. J. For. Res. 38, 1661–1675.

Zhang, K.Q., Liu, H.Q., Li, Y.P., Xu, H.Z., Shen, J., Rhome, J., Smith, T.J., 2012. The role of mangroves in attenuating storm surges. Estuar. Coast. Shelf Sci. 102, 11–23.

Zianis, D., 2008. Predicting mean aboveground forest biomass and its associated variance. For. Ecol. Manage. 256, 1400–1407.

Zianis, D., Mencuccini, M., 2004. On simplifying allometric analyses of forest biomass. For. Ecol. Manage. 187, 311–332.